Attenuation and dispersion of first sound near the superfluid transition of pressurized ^{4}He

R. Carey,* Ch. Buchal, and F. Pobell
Institut für Festkörperforschung, Kernforschungsanlage Jülich, 517 Jülich, West Germany
(Received 25 April 1977)

The attenuation α, the velocity u, and the dispersion $D = u(\omega) - u(0)$ of first sound have been measured in pressurized liquid ^{4}He ($P = 0.06$, 5.01, 9.21, 15.24, 20.38, 25.46, 29.33 bar) near the superfluid transition. The frequency range was 4.6 kHz $\leq \omega/2\pi \leq$ 1.0 MHz, the temperature range was 1 μK $\leq |T - T_\lambda| \leq$ 3 mK. From the measured velocities we calculate the thermodynamic velocity $u(0)$, as well as $(\partial S/\partial P)_\lambda$ and $(\partial V/\partial P)_\lambda$. The attenuation and the dispersion at constant $T_\lambda - T$ are only weakly pressure dependent. They are interpreted as arising from a relaxation process occurring only below T_λ, and a fluctuation process occurring on both sides of the λ transition; both contributions have about equal strength. The strength A_R of the relaxation process and the amplitude τ'_0 of the relaxation time $\tau' = \tau'_0 t^{-x'}$ are independent of pressure to within 10%; ($t = |T - T_\lambda|/T_\lambda$). The latter result seems to be inconsistent with the pressure independence of the correlation-length amplitude $\xi'_0 = 1.0 \pm 0.05$ Å (which was confirmed in this work), and the known pressure dependence of the amplitude $u_{2,0}$ of second-sound velocity, if the relation $\tau' = \xi'/u_2$ is correct. For $T > T_\lambda$, where only critical fluctuations contribute, our absorption and dispersion data for all ω and P can be scaled with functions of $\omega\tau$ for $10^2 > \omega\tau > 10^{-2}$. This scaling analysis shows that the time τ characterizing the critical order-parameter fluctuations at $T > T_\lambda$ has the same temperature and pressure dependence as the relaxation time τ' at $T < T_\lambda$; these two times differ at most by a constant multiplicative factor. Below T_λ, the data are represented by the sum of the contribution represented by the scaling function plus the contribution from order-parameter relaxation. The weak pressure dependence of α and D, and the pressure independence of A_R, ξ'_0, τ'_0, and τ_0 contrasts with the strong concentration dependence of these quantities in ^{3}He-^{4}He mixtures. The scaling functions determined from our data are identical in form to those determined earlier from the mixture data. The frequency dependences of the attenuation and of the dispersion for $\omega\tau \gtrsim 1$ scale as $\alpha \propto \omega^{1+y}$ and $D \propto \omega^y$, respectively, with $y = 0.15 \pm 0.03$.

I. INTRODUCTION

The dynamics of the superfluid phase transition of liquid helium can be studied by investigating the velocity u and attenuation α of first sound. Precise measurements of the dispersion $u(\omega) - u(0)$ and of the attenuation $\alpha(\omega)$ allow the determination of the time scale characterizing this phase transition. Such measurements have been performed for ^{4}He,[1-4] and for ^{3}He-^{4}He mixtures under saturated vapor pressure.[5-8] The results of these experiments verified several theoretical predictions[9-15] for the superfluid transition. In this paper we report on a systematic study of the velocity, dispersion and attenuation of low-frequency first sound in pressurized liquid ^{4}He along the λ line. The special interest in studying critical phenomena as a function of ^{3}He concentration X_3 or pressure P results from the fact that these are "invert" variables for the superfluid transition. Therefore, according to the universality concept, they should leave critical exponents and amplitude ratios unchanged.[16-21] Furthermore, the pressure and temperature dependence of the second-sound velocity u_2,[22] of the superfluid density ρ_s/ρ,[22] of the healing length ξ_H,[23] of the specific heat C_p,[24] and of the thermal-expansion coefficient[25] β_p have all been carefully studied in ^{4}He near $T_\lambda(P)$. This enables us to perform a thorough analysis of our data and to calculate thermodynamic parameters from them.

The paper is organized in several sections paralleling the paper of Buchal and Pobell (BP) which contains a more thorough presentation of experimental details.[6] Section II gives a summary of theoretical predictions. In Sec. III we describe the apparatus, the pressure regulating system, and the experimental procedure. In Sec. IV we present the data of the sound velocity, dispersion, and attenuation. We calculate the thermodynamic velocity of sound $u(0)$, $(\partial S/\partial P)_\lambda$, and $(\partial V/\partial P)_\lambda$ for various P. Section V contains the discussion and interpretation of the dispersion D and attenuation α. A summary and conclusions are given in Sec. VI. In the appendix we discuss the influence of confluent singular terms in the used equations.

II. THEORY

The theory of sound propagation near T_λ has been presented in detail by a number of authors.[9-15,26-28] A summary of the relevant physical considerations is given in BP.[6] Here we present only those equations which are important for the following analysis.

A. Thermodynamic velocity of sound

For $\omega = 0$ and in the limit $T \to T_\lambda$ the relation

$$u^*(0) = aC_p^{-1} + bt + c \tag{1}$$

becomes exact. Here $u^*(0)$ is the thermodynamic velocity, the asterisk denotes a zero-height sample, a, b, c, are constants with $a = (u_\lambda^{*3} T_\lambda / 2V_\lambda^2)(\partial S/\partial P)_\lambda^2$, and $t = |T - T_\lambda|/T_\lambda$. Because of the sharp peak in the specific heat C_p, $u^*(0)$ has a sharp minimum at T_λ which becomes more pronounced at higher pressures. Equation (1) has been found to describe the values for $u^*(0)$ at saturated vapor pressure (SVP) very well.[1,6,26]

B. Dispersion and attenuation of sound

At finite frequencies the velocity becomes frequency dependent, and a pronounced increase in the sound attenuation occurs near T_λ. Paralleling the discussion of sound at SVP,[2-8,11] we discuss our attenuation and dispersion data in terms of two processes, order-parameter relaxation and order-parameter fluctuations. Doing so, we use primed parameters at $T < T_\lambda$; unprimed parameters are used at $T > T_\lambda$, if they pertain to both phases, or in obvious cases. We will only discuss the contributions associated with the superfluid transition, neglecting the "background" attenuation and dispersion, which change insignificantly with temperature in the investigated t range.

1. Order-parameter relaxation

Landau and Khalatnikov have shown that the superfluid density ρ_s, when disturbed from equilibrium by a pressure wave, requires a relaxation time τ' to adjust to the changing pressure in the sound wave.[9-12] The relaxation occurs only below T_λ where the time average of the order parameter is nonzero. If a single relaxation time τ' is involved, the resulting attenuation α_R and dispersion D_R are given by

$$\alpha_R = (\Delta u/u^2)\omega^2\tau'/(1+\omega^2\tau'^2),$$
$$D_R = \Delta u \omega^2 \tau'^2/(1+\omega^2\tau'^2). \tag{2}$$

The relaxation time

$$\tau' = \tau_0' t^{-x'} \tag{3a}$$

should be given by

$$\tau' = \xi'/u_2 \tag{3b}$$

(ξ' is the correlation length; u_2 is the velocity of second sound).[10-12] With the proportionality $\xi' \propto \rho_s^{-1}$,[14,19,20] we have a critical exponent of 0.675 for[22,25] ξ'. The critical exponent of u_2 has been determined as 0.387,[29] so we find $x' = 1.062$. A different exponent x' is discussed in the Appendix. The relation for $\Delta u = u(\infty) - u(0)$ has been derived in Refs. 11 and 12. Hohenberg's result is

$$\Delta u = \frac{u^3 \rho k_B T}{4\pi\xi'^3}\left[\frac{\rho}{\rho_s}\frac{\partial(\rho_s/\rho)}{\partial T}\frac{T}{C_p}\left(\frac{\partial S}{\partial P}\right)_\lambda\right]^2. \tag{4}$$

The temperature dependence of Δu is then given by

$$\Delta u = A_R C_p^{-2} t^{3\nu'-2}, \tag{5}$$

where ν' is the critical exponent of the correlation length, and A_R is a constant.[3,6] Using a scaling law,[30] and recent data for the specific heat exponent α',[25] we have $3\nu' - 2 = -\alpha' = 0.026$. Furthermore we use

$$A_R = \frac{u^3 \rho k_B T \xi^2}{4\pi\xi_0'^3}\left(\frac{\partial S}{\partial P}\right)_\lambda^2, \tag{6}$$

where ξ is the critical exponent of ρ_s, 0.675.[22,25] For the specific heat we use

$$C_p = (A'/\alpha')t^{-\alpha'}(1 + D' t^{z'}) + B', \tag{7}$$

with universal exponents $\alpha' = -0.026$ and $z' = 0.5$.[25] For the pressure-dependent coefficients A', D', and B' we use values reported in Refs. 24 and 25. For an analysis of our data with equations using confluent singular next-order terms in t see the Appendix.

2. Order-parameter fluctuations

There is a coupling of the sound wave to critical fluctuations of the order parameter. This occurs on both sides of T_λ, is nonsingular at T_λ, and has been discussed for the superfluid transition in several theoretical papers,[11,13-15,28] without giving a result to which our data could be compared in detail. The recent first principle calculations on the dynamics of the superfluid transition[19,20] do not treat sound propagation. The sound absorption α_F due to fluctuations above and below T_λ is expected to be about equal for the same values of t, and to be of about the same strength as the relaxation contribution.[11] This has been confirmed experimentally in Ref. 6. According to universality,[16-21] the ratio α_F/α_F' should be pressure independent, and α_F and α_F' should have the same t dependence. The scaling prediction of Kawasaki for this process,[15] as discussed by BP,[6] may be written for the attenuation as

$$\alpha_F = B_F t^s \omega F(\omega\tau) = C_F \omega^{1+s/x} f(\omega\tau), \tag{8}$$

where s is a small positive number, and B_F and C_F are constants only depending on pressure. Here $\tau = \tau_0 t^{-x}$ is the time characterizing the critical order parameter dynamics. Dynamic scaling predicts that τ diverges the same way above and below T_λ,[11,13-15] and the ratio of its amplitudes above and below T_λ should be pressure independent.[16-21] τ is not *a priori* identical to the relaxation time τ'.

The exponent $1+s/x$ is only slightly greater than 1. Kroll has recently performed a calculation of the critical attenuation above T_λ using mode-mode coupling and renormalization group theory.[28] But he does not state an analytic form for the scaling function $f(\omega\tau)$. Thus we will only compare our data to numerical results by Kroll. The validity of Eq. (8) is restricted to the range where the sound wavelength is much greater than the range of correlations of critical fluctuations ($\omega\tau \ll u/u_2$). This condition is always fulfilled for our measurements.

3. *Hydrodynamic regime*

In the hydrodynamic regime ($\omega\tau \ll 1$) the attenuation and dispersion vary as

$$\alpha \propto \omega^2 \quad \text{and} \quad D \propto \omega^2 . \tag{9}$$

Equations (2) and (8) have to merge into this form for $\omega\tau \ll 1$. In the regime $\omega\tau \lesssim 0.1$ our data lose accuracy, because α and D become rather small. In addition, the hydrodynamic losses are only very weakly temperature dependent in our temperature range and become part of a constant background which has to be subtracted from the measured attenuation. Consequently, the hydrodynamic behavior was not investigated in detail in this work, but our data are consistent with Eq. (9) for $\omega\tau \lesssim 0.1$.

III. EXPERIMENTAL

A. Cryogenics and resonators

A schematic diagram of the cryogenic apparatus is shown in Fig. 1. A detailed description has been given in BP[6] except for the pressure regulating system (see below). Our sample chamber contains

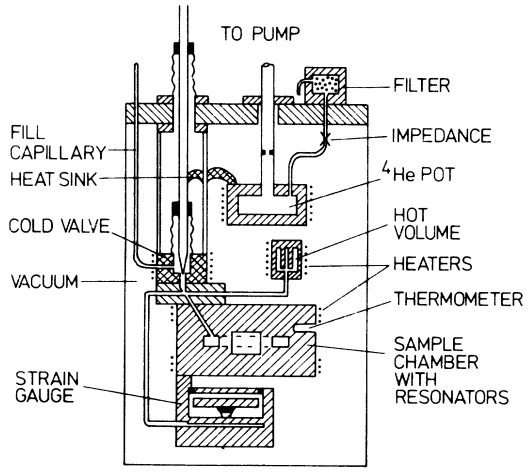

FIG. 1. Cryogenic part of the experimental apparatus.

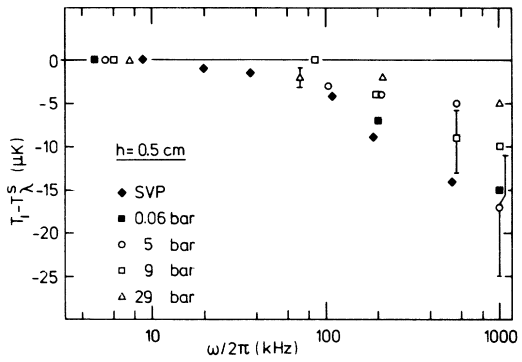

FIG. 2. Temperature difference $T_i - T_\lambda^s$ as a function of sound frequency for the indicated pressures. Here T_i is the temperature at which the velocity of sound has its inflection point (see Figs. 3 and 4); T_λ^s is the temperature at which the λ transition reaches the top of our 0.5-cm high sample. The value $T_i - T_\lambda^s$ is set equal to zero at $\omega/2\pi \to 0$. The data at SVP are from Ref. 6.

two sound resonators. Hence, we can take data simultaneously under identical conditions at two different frequencies. In both resonators sound was excited and detected by condenser transducers whose active elements were mylar foils.[1-3,5,6] Principal advantages of the system are its low height (0.5 cm), thus limiting the influence of gravity,[31] and the use of a torus resonator as an acoustic thermometer, i.e., as a λ-point detector (see below and Fig. 2).[2,3,5,6] The cylinder resonator has a fundamental plane wave harmonic of 21 kHz at SVP, and 35 kHz at $P=29$ bar. It was used for frequencies up to 1 MHz.

The sample thermometer was a commercial germanium resistor,[32] calibrated against the 1958 ^{4}He vapor pressure scale, and measured in a standard ac-bridge arrangement.[23,25] Only 1 nW of heat was dissipated in the thermometer resulting in negligible self-heating. Temperature changes of 0.5 μK could be resolved, and the temperature of the copper chamber was regulated to within this limit. From the behavior of the sound velocity we determined T_λ.[2,3,5,6] The combination of the pressure dependence $(\partial T/\partial P)_\lambda$ of the superfluid transition, and the finite height h of the sample, across which there exists a gravitational pressure gradient, induces a λ temperature T_λ^s at the top of the sample which is higher by $\rho g h(\partial T/\partial P)_\lambda$ than the transition temperature T_λ^b at the bottom of the sample.[31] This leads to the inflection point of $u(0)$ at T_λ^s.[3,5,6,26] With increasing frequency this inflection point occurs at slightly lower temperatures T_i,[6] as shown in Fig. 2; for $\omega/2\pi \lesssim 10$ kHz, $|T_i - T_\lambda^s|$ is less than our resolution of 0.5 μK. During each run we used the inflection point of the second harmonic of the torus resonator, with frequency $\omega/2\pi = f_{T_2}$, to deter-

mine T_i, and we refer all of our temperatures to this value. We have $4.6 \leq f_{T2} \leq 7.4$ kHz at $0.06 \leq P \leq 29.33$ bar. We believe our determination of $T - T_\lambda^s$ is accurate to better than 1 μK. Thus, T_λ^s is a measured quantity, and not a free parameter in the data analysis.

The electronic setup and the detailed performance of the sound detection system have been described in BP.[6] The rapid phase change of the pickup signal near a resonance was used to track that resonance as the temperature and hence the resonant frequency drifted. The stability of the feedback system allowed velocity changes of $\Delta u/u \simeq 10^{-6}$ to be measured. However, the repeatability of individual frequency measurements was limited by the quality $Q = \omega_0/\Delta\omega(-3\text{ dB})$ of the resonances. We estimate our stability and reproducibility of ω_0 to about 0.02 $\Delta\omega$. The tracking ability of the system is also limited by this factor. A representative error then for $Q = 1000$ is $\Delta u \simeq 0.5$ cm/sec or $\Delta u/u \simeq 20$ ppm.

B. Pressure regulation and procedure

The operation of a strain gauge–hot volume pressure regulating system has been thoroughly discussed by Ihas and Pobell,[23] and by Mueller, Ahlers, and Pobell.[25] Briefly, the strain gauge, thermally attached to the sample chamber, senses pressure deviations which are detected as an error signal in a capacitance bridge circuit. The error signal is amplified, integrated, and fed back into a heater on the hot volume, forcing liquid into or out of the sample chamber. This maintains the pressure constant. The hot volume can be operated in the range 2.5–10 K without affecting the stability of the system ($\Delta P/P \simeq 10^{-7}$). An additional thermal link of about 100 μW/K between the sample chamber and the ^{4}He pot was installed to balance the heat flow along the helium-filled capillary between hot volume and sample.

The strain gauge was calibrated against a previously calibrated Heise bourdon-tube pressure gauge over the range $5 \leq P \leq 25$ bar. The capacitance C of the strain gauge is well represented by $1/C = A_0 + A_1 P + A_2 P^2$. We measured a capacitance of 38 pF at 1 bar and of 130 pF at 29 bar. For each pressure the sample chamber was filled through the fill capillary to the approximate pressure, then the cold valve was closed, and the capillary above the valve was evacuated. After that, the pressure was adjusted by varying the temperature of the hot volume. After all data were taken, the strain gauge was again calibrated in the ranges of ±0.5 bar around the used pressures, confirming the stability of the capacitive manometer. Data were taken at constant pressure, either with the temperature also held constant to within 0.5 μK, or during drifts of about 2 μK/min. While the temperature drifted, the resonant frequencies of both resonators, one sound amplitude, and the temperature were recorded on a four-pen recorder. Simultaneously, one resonant frequency, its amplitude, and the temperature were recorded automatically and stored on magnetic tape. When the temperature was held constant, the frequencies at the −3-dB points of the particular resonance were also measured. These data give the Q value and the total absorption, via $Q = \omega_0/\Delta\omega(-3\text{dB})$, and $\alpha_{\text{expt}} = \omega_0/2Qu$. Far away from T_λ, our resonators had Q values of 130–3000, depending on resonator and frequency, decreasing to 100–500 near T_λ. Comparing the Q values with the amplitudes U of the resonances, we found that near T_λ, Q is proportional to U. We then used this relation for calculating α_{expt} in the region where the temperature drifted, and the amplitude was recorded continuously to obtain continuous curves for the absorption coefficient. From the measured attenuation α_{expt} we subtracted a constant effective background attenuation α_B measured far away from T_λ in order to obtain the attenuation $\alpha = \alpha_{\text{expt}} - \alpha_B$ associated with the λ transition. In this constant background α_B the wall losses as well as the very weakly temperature-dependent part of the hydrodynamic attenuation are included. The ratio $\alpha_B/\alpha_{\text{expt, max}}$ was less than 0.1 at 1 MHz and became as high as 0.8 for the low-frequency resonances in the torus. The electrical crosstalk was normally less than 1% of the pickup signal.

We measured the frequency and amplitude of the sound velocity versus temperature at $\omega/2\pi \simeq f_{T2}$, 100, 200, 600 and 1000 kHz at the various pressures.[33] For each run involving one of the four high frequencies, the velocity of the low-frequency torus resonance at f_{T2} was also recorded, providing an accurate λ temperature, independent of the germanium resistor.

IV. EXPERIMENTAL RESULTS (REF. 34) AND ANALYSIS OF THERMODYNAMIC VELOCITY

A. Influence of gravity

The λ transition is pressure sensitive with a slope $(\partial T/\partial P)_\lambda < 0$. For a sample of finite height the gravity-induced pressure gradient leads to a lower T_λ at the bottom than at the top of the cell.[31] The absolute value of the slope $(\partial T/\partial P)_\lambda$ of the λ line increases with pressure.[35] For a 0.5-cm high sample the spread in transition temperature ranges from 0.6 μK at saturated vapor pressure to 1.6 μK at $P = 29$ bar. Further, as the pressure is increased, and particularly at $T \gtrsim T_\lambda$, the temperature dependence of the sound velocity in-

creases. In the most severe case ($P = 29$ bar), the sound velocity varies by 0.5 cm/sec over the height of the resonator even at $T - T_\lambda \simeq 100$ μK. For this case only, some low-frequency measurements are slightly influenced by gravity even for $T - T_\lambda \lesssim 100$ μK.

B. Sound velocity and related thermodynamic parameters

Our measurements of resonant frequencies of the helium-filled cavities are more precise than the determination of the cavity length, including a necessary correction for the moving transducer foils at the ends. To convert frequency to sound velocity we therefore normalized the data at $P = 0.06$ bar for $\omega/2\pi = 4.6$ kHz to the value $u(0) = 21808$ cm/sec at $T - T_\lambda^s = -40$ μK. This value extrapolates to $u(0) = 21800$ cm/sec at SVP and $T - T_\lambda^s = -40$ μK, in agreement with BP.[6] At this temperature and pressure, dispersion and gravity effects are negligible, and the velocity is only mildly temperature dependent (0.2 cm/sec μK). From our normalization value we obtain $u_\lambda^*(0) = 21751$ cm/sec at $P = 0.06$ bar, where $u_\lambda^*(0)$ is the value of the thermodynamic velocity in a zero-height sample at T_λ. Interpolating to SVP we find $u_\lambda^*(0) = 21743$ cm/sec, a slightly higher value than found by previous authors.[1,3,6,26] This difference is the result of the different C_p functions used in the analysis (see below).[6,24,25] In each run the second harmonic of the torus resonator with frequency f_{T2} was recorded. The frequency of a resonance in the cylinder resonator was normalized to the low-frequency data at a temperature far enough below T_λ such that no dispersion effects were present. Hence all of our velocity data are normalized to $u(0) = 21800$ cm/sec at SVP and $T - T_\lambda^s = -40$ μK. Examples of the sound velocity are shown in Fig. 3 for three frequencies at each of three different pressures. The velocity scales are referenced to $u_\lambda^*(0)$ (see Table I).

The values of the velocity of sound determined from the low-frequency torus resonances were fit to Eq. (1) over the temperature range $\Delta T_L \leq |T - T_\lambda^s| \leq 1$ mK for $20 \leq \Delta T_L \leq 100$ μK. The limiting temperature difference ΔT_L at which our data became sensitive to the effect of gravity was determined from the difference $T_\lambda^b - T_\lambda^s = \rho g h (\partial T/\partial P)_\lambda$, ($h = 0.5$ cm), the slope of the velocity data (du/dT), and an assumed resolution of 0.15 cm/sec. For these temperatures and low frequencies f_{T2} there is no dispersion of sound. The fits were performed independently for $T < T_\lambda$ and $T > T_\lambda$. For the specific heat we used Eq. (7) with parameters determined from the thermal expansion coefficient results of Mueller, Ahlers, and Pobell,[25] and, at SVP, those of Van Degrift,[36] along

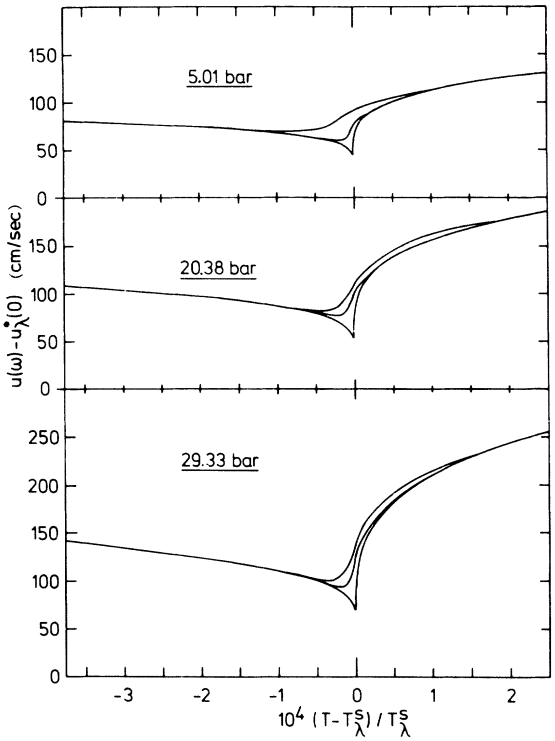

FIG. 3. Measured first sound velocity $u(\omega) - u_\lambda^*(0)$ as a function of $(T - T_\lambda^s)/T_\lambda^s$ for the three indicated pressures. The data are for $\omega/2\pi = 1005$, 206, and 5.5 kHz for $P = 5.01$ bar; for $\omega/2\pi = 1018$, 196, and 7.0 kHz for $P = 20.38$ bar; for $\omega/2\pi = 1020$, 211, and 7.4 kHz for $P = 29.33$ bar. $u_\lambda^*(0)$ is the thermodynamic velocity at T_λ in a sample of zero height, as given in Table I.

with the relation $C_p = VT\beta_p + T\partial S/\partial T$. At all pressures the differences $u_{\text{measured}} - u_{\text{fit}}$ were generally less than 0.1 cm/sec over the fitted range of temperature. The mean values $u_\lambda^*(0)$ calculated from the fits at $T < T_\lambda$ and at $T > T_\lambda$ are given in Table I. They are consistently higher than the values calculated from thermodynamic parameters by Ahlers,[24] with a difference increasing with pressure from about 0.4 m/sec at SVP to about 7 m/sec at 25 bar.[37] Our values for $u_\lambda^*(0)$ depend on the equation used for the t dependence of C_p. But even assuming a logarithmic t dependence with the coefficients given in Ref. 24, our values for $u_\lambda^*(0)$ decrease by only 20–40 cm/sec. Therefore, we find good agreement with the values for $u_\lambda^*(0)$ at SVP as published by Refs. 1, 3, 6 and 26, but we have no explanation for the discrepancies increasing with pressure between our values and those given in Refs. 24 and 37. Table I also contains values for the difference between the minimum thermodynamic velocity in a sample of 0.5-cm height and the minimum thermodynamic velocity in a sample of zero height at T_λ, $u_{\min}(0)$

TABLE I. Thermodynamic velocity, related parameters, and dispersion.

P (bar)	0.06	5.01	9.21	15.24	20.38	25.46	29.33
T_λ (K)	2.171	2.122	2.073	1.995	1.922	1.842	1.775
f_{T2} (kHz) [a]	4.6	5.5	6.0	6.6	7.0	7.2	7.4
$u^*_\lambda(0)$ (cm/sec) [b,c]	21751	25583	27987	30735	32579	34029	34871
$u_{min}(0) - u^*_\lambda(0)$ (cm/sec) [c,d]	38	42	42	44	47	52	63
$u_{min}(f_{T2}) - u^*_\lambda(0)$ (cm/sec) [e]	47	53	56	53	55	62	79
$u(1.0\ \text{MHz}, T_\lambda) - u^*_\lambda(0)$ (cm/sec) [f]	79	82	89	92	88	117	117
$\left(\frac{\partial S}{\partial P}\right)_\lambda \left(\frac{\text{cm}^3}{\text{mole K}}\right)$	−0.95	−0.71	−0.59	−0.51	−0.47	−0.46	−0.48
$10^7\left(\frac{\partial V}{\partial P}\right)_\lambda \left(\frac{\text{cm}^5}{\text{mole dyne}}\right)$	−3.88	−2.47	−1.91	−1.44	−1.20	−1.03	−0.93

[a] f_{T2} is the frequency of the second harmonic in the torus resonator.
[b] Thermodynamic velocity in a zero-height sample normalized at $u^*(0) = 21\,800.0$ cm/sec for SVP at $T - T^s_\lambda = -40\ \mu$K.
[c] Using Eq. (7) for C_p.
[d] $u_{min}(0)$ is the minimum thermodynamic velocity for a 0.5-cm-high sample.
[e] $u_{min}(f_{T2})$ is the minimum velocity measured at f_{T2} in our 0.5-cm-high sample.
[f] $u(1.0\ \text{MHz}, T_\lambda)$ is the sound velocity measured at 1.0 MHz, which is not noticeably influenced by gravity.

$- u^*_\lambda(0)$. The quantity $u_{min}(0)$ is obtained from the mentioned fits to Eq. (1) and by using $\rho g h(\partial T/\partial P)_\lambda = 0.60$, 0.86, 0.98, 1.15, 1.29, 1.45, and 1.60 μK for $P = 0.06$, 5.01, 9.21, 15.24, 20.38, 25.46, and 29.33 bar, respectively, for the calculation of the influence of gravity on $u^*(0)$ close to T_λ.[26] We attribute the difference for the value $u_{min}(0) - u^*_\lambda(0)$ obtained here at $P = 0.06$ bar and the values obtained in earlier work at SVP[6,26] to the different equations used for C_p. In addition, Table I contains $u_{min}(f_{T2}) - u^*_\lambda(0)$, where $u_{min}(f_{T2})$ is the minimum velocity measured at the second harmonic of the torus resonator. This difference increases by about 70% with increasing pressure, whereas it decreased by two orders of magnitude in ^{3}He-^{4}He mixtures.[6] To compare the zero-height thermodynamic velocity $u^*(0)$, the thermodynamic velocity $u(0)$ in our 0.5-cm-high sample, and the velocity $u(f_{T2})$ measured at our lowest frequency we show in Fig. 4 these three velocities very near T^s_λ at $P = 15.21$ bar. For the thermodynamic velocity at T_λ we find that the empirical relation

$$u^*_\lambda(0) = 391.1 - 173.3\ e^{-0.48P}\ (\text{m/sec}), \qquad (10)$$

with P in bar, fits our measured values to within $\Delta u/u \lesssim 0.5\%$. From the values for the coefficient a of Eq. (1), which is related to thermodynamic quantities, we calculate $(\partial S/\partial P)_\lambda$, using published data for V_λ,[24] and our data for T_λ and $u^*_\lambda(0)$, (see Table I). The values obtained from data at $T > T_\lambda$ and at $T < T_\lambda$ are shown as a function of P in Fig. 5. The two values at each P agree within their errors, and they agree well with earlier published values at SVP.[6,26] The difference $(\partial S/\partial P)^+_\lambda - (\partial S/\partial P)^-_\lambda$ is not as large as observed in the mixtures by BP, an improvement attributable to the improved specific-heat function used in this analysis. The values for $|(\partial S/\partial P)_\lambda|$ decrease with pres-

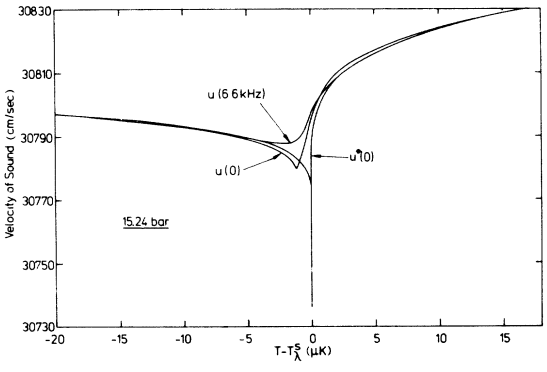

FIG. 4. Velocity of sound very near T^s_λ. The velocity u (6.6 kHz) is the sound velocity at $\omega/2\pi = 6.6$ kHz measured in our 0.5-cm-high sample; $u^*(0)$ is the thermodynamic sound velocity in a zero-height sample computed with Eq. (1) from a fit to our data for u (6.6 kHz) at $|T - T^s_\lambda| > 20\ \mu$K; $u(0)$ is the thermodynamic sound velocity in our 0.5-cm-high sample computed with the relation $T^b_\lambda - T^s_\lambda = \rho g h(\partial T/\partial P)_\lambda$ and $u^*(0)$. All velocities are normalized to $u(0) = 21800$ cm/sec at SVP and $T - T^s_\lambda = -40\ \mu$K.

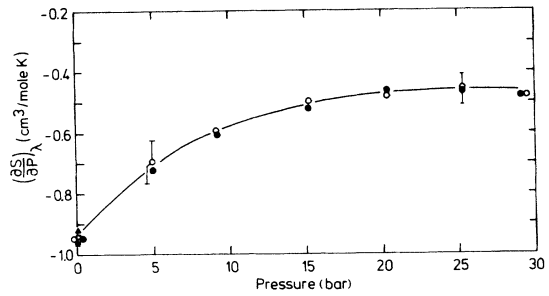

FIG. 5. $(\partial S/\partial P)_\lambda$ vs pressure. The values shown are calculated from the parameter a of Eq. (1) which has been obtained from fits of Eq. (1) to the low-frequency sound data measured at $T<T_\lambda$ (●), and at $T>T_\lambda(0)$. The squares and the triangle at SVP are from Refs. 6 and 26, respectively. The error bars shown are typical and correspond to the deviation of the fitted parameter a of Eq. (1) resulting from an error of 0.3 cm/sec in the sound velocity. The solid line is a guide for the eye only.

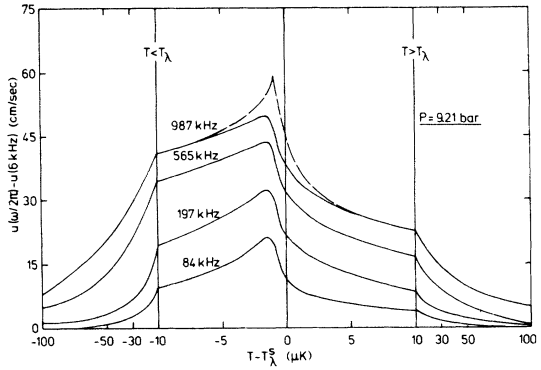

FIG. 6. Measured velocity difference $u(\omega/2\pi)-u(6$ kHz) for $P=9.21$ bar and the frequencies shown, as a function of $T-T_\lambda^s$. The dispersion $u(6\text{ kHz})-u(0)$ which must be added to each of the shown curves to obtain the dispersion $u(\omega/2\pi)-u(0)$ is the dashed peak on top of the highest-frequency curve. Note the changes in temperature scale at $|T-T_\lambda^s|=10\ \mu$K.

sure by about a factor of 2 from $P=0$ to 18 bar and then are almost constant from $P=18$ to 29 bar.

With the relation[6,26]

$$\left(\frac{\partial V}{\partial P}\right)_\lambda = -\left(\frac{V_\lambda}{u_\lambda^*}\right)^2 + \left(\frac{\partial T}{\partial P}\right)_\lambda \left(\frac{\partial S}{\partial P}\right)_\lambda - \frac{T}{C_p}\left(\frac{\partial S}{\partial P}\right)^2, \tag{11}$$

where all quantities are per unit mass, we calculate $(\partial V/\partial P)_\lambda$. As shown in Table I, the values for $|(\partial V/\partial P)_\lambda|$ decrease by a factor of 4 when the pressure is increased to 29 bar. We used V_λ given by Ahlers,[24] C_p from the β_p data of Mueller, Ahlers, and Pobell,[25] $(\partial T/\partial P)_\lambda$ from Kierstead,[34] and our data for u_λ and $(\partial S/\partial P)_\lambda$.

C. Dispersion

At finite ω the dip in u near T_λ becomes less distinct due dispersion of sound.[3,5,6] Figure 3 already demonstrates that this dispersion does not depend much upon pressure, in contrast to the strong concentration dependence observed in mixtures.[6] One may also see that the minimum in u, which for $\omega=0$ occurs at T_λ^b,[26] moves away from T_λ with increasing ω.[3,6]

From the velocity data we determined $u(\omega/2\pi)-u(f_{T_2})$ and the sound dispersion $D=u(\omega)-u(0)$. The frequency dependence of these two quantities at all pressures is very similar to that at SVP[3] and to that in the mixtures[6] (see Fig. 6). In Fig. 7 we show the dispersion D at $\omega/2\pi=1.0$ MHz for three pressures. There is a trend toward higher dispersion at higher pressures. But whereas the dispersion decreased by about a factor of 20 in the mixtures between $X_3=0$ and $X_3=0.52$ near T_λ, it increases by less than a factor of 2 with increasing pressure. The measured dispersion is asymmetric around T_λ^s with a peak on the low-temperature side. The maximum of the dispersion occurs slightly below T_λ^s because we used a sample of finite height, and refer all temperatures to the temperature T_λ^s for which the transition occurs at the top of the sample. Even at $\omega/2\pi=f_{T_2}$ there is measurable dispersion at $|T_\lambda^s-T|<5\ \mu$K (see Figs. 4 and 6). For the evaluation of the dispersion $D=u(f_{T_2})-u(0)$ a precise determination of $u(0)$, and therefore C_p is necessary. As there are no sufficiently precise experimental C_p data at $|T_\lambda^s-T|<5\ \mu$K available, we prefer to analyze the dispersion in the region where $u(f_{T_2})-u(0)=0$, i.e., for $|T-T_\lambda^s|>5\ \mu$K. The frequency f_{T_2} is so low, and the height of our sample is so small that $u(\omega/2\pi)-u(f_{T_2})$ represent the dispersion D with sufficient accuracy for $|T-T_\lambda^s|>5\ \mu$K.

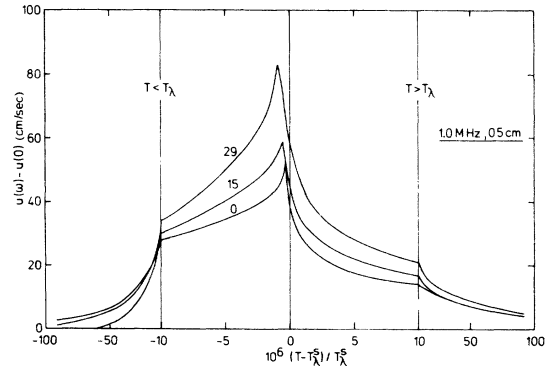

FIG. 7. Dispersion $u(1\text{ MHz})-u(0)$ at three pressures as a function of $t=(T-T_\lambda^s)/T_\lambda^s$. Note the changes in scale at $|t|=10^{-5}$.

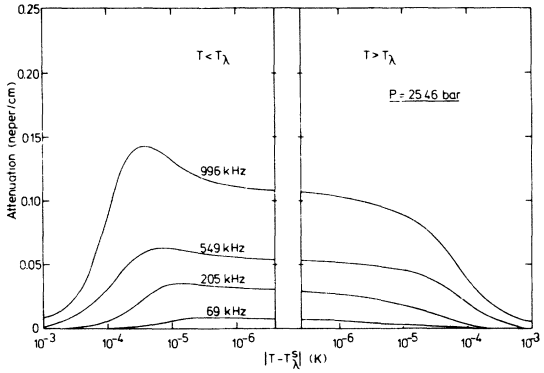

FIG. 8. Attenuation at $P = 25.46$ bar for the given frequencies as a function of $|T - T_\lambda^s|$. A temperature-independent background has been subtracted.

D. Attenuation

In Fig. 8 we show as an example the frequency dependence of the attentuation at $P = 25.46$ bar. The attenuation at $\omega/2\pi = 1.0$ MHz at various pressures is shown in Fig. 9. The attenuation α, too, is asymmetric about T_λ^s with a peak in the superfluid phase. It is a smooth nonsingular function of t. The position of the maximum in α moves away from T_λ^s with increasing ω, but appears at the same $t = (T - T_\lambda^s)/T_\lambda^s$ for a constant ω and all pressures. This latter behavior again is strikingly different from that in the mixtures where the maximum moves away from T_λ^s with increasing X_3.[6] The pressure dependence of the strength of the attenuation maximum and of the attenuation near T_λ are shown in Fig. 10. They both decrease slightly from $P = 0$ to 10 bar and are nearly constant from $P = 10$ to 25 bar. A common feature of attenuation and dispersion is their weak pressure dependence compared to the strong concentration dependence observed in the mixtures.[6] But we observe in

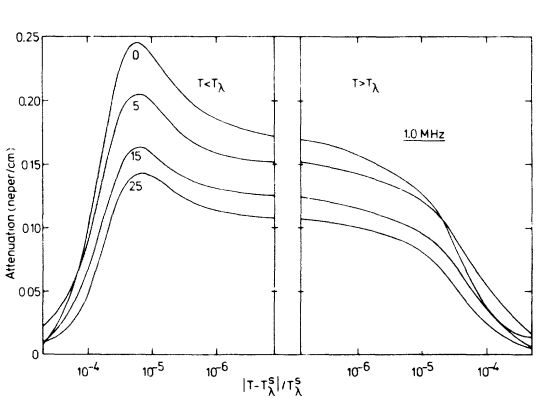

FIG. 9. Attenuation at $\omega/2\pi = 1.0$ MHz for the indicated pressures as a function of $|T - T_\lambda^s|/T_\lambda^s$. A temperature-independent background has been subtracted.

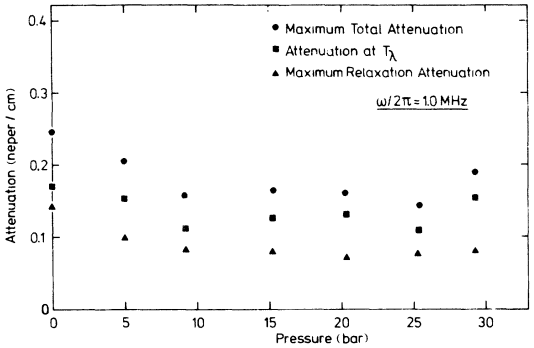

FIG. 10. Values of the indicated attenuations at $\omega/2\pi = 1.0$ MHz as a function of pressure

Figs. 7 and 9 that $\alpha(P)$ and $D(P)$ are changing in opposite senses as the pressure is increased. This results from the factor u^{-2} in Eq. (2) for the damping which decreases strongly with increasing pressure. The temperature dependence of the attenuation near T_λ is very weak (see Figs. 8 and 9). Hence for the analysis of the attenuation we can use data in the range $|T - T_\lambda^s| > 1$ μK.

V. ANALYSIS AND INTERPRETATION OF THE DATA FOR DISPERSION AND ATTENUATION OF SOUND

A. Attenuation and dispersion due to relaxation

In our temperature and frequency range the attenuation and dispersion of sound near T_λ are arising from order-parameter relaxation below T_λ and order-parameter fluctuations on both sides of T_λ. The processes are assumed to be additive.[2-8] According to scaling,[30] the fluctuation contribution should have the same t dependence on both sides of T_λ. Also, according to the universality concept, the ratio of the fluctuation contributions above and below T_λ on an appropriate temperature scale is expected to be independent of the inert variable "pressure."[16-21] These predictions are inherent in the scaling form, Eq. (8). Buchal and Pobell have discussed in detail the data for the attenuation and dispersion at SVP and in mixtures of ^{3}He – ^{4}He. They found that those data are well described, assuming that the absolute value of the fluctuation contribution to α and D above and below T_λ at the same t are about equal; no improvement in the fits of the data was obtained by avoiding this assumption.[6] This assumption was first applied by Williams and Rudnick.[2] Assuming this equality again, we have,

$$\alpha(T > T_\lambda) = \alpha_F\,, \qquad \alpha(T < T_\lambda) = \alpha_F + \alpha_R\,. \tag{12}$$

Therefore,

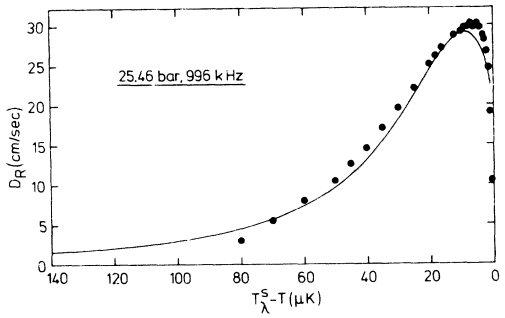

FIG. 11. Relaxation part D_R of the dispersion as a function of $T_\lambda^s - T$ for $P = 25.46$ bar and $\omega/2\pi = 996$ kHz. The data points were determined from continuous measurements and are the difference between the dispersion measured below and above T_λ^s. The full line is a fit of Eq. (2) with Eqs. (3a) and (5) to the data shown at $T_\lambda^s - T \geq 5$ μK with $x' = 1.062$, and A_R and τ_0' as free parameters.

$$\alpha_R = \alpha(T < T_\lambda) - \alpha(T > T_\lambda),$$

and, correspondingly, (13)

$$D_R = D(T < T_\lambda) - D(T > T_\lambda).$$

The experimental results for α_R and D_R, as obtained by the above equations were fit to the equations given in Sec. II B for the attenuation and dispersion due to relaxation only. Attenuation data for $|T - T_\lambda^s| > 1$ μK and dispersion data for $|T - T_\lambda^s| > 5$ μK were fit independently for each frequency and pressure. The fits were performed with Eqs. (2), (3a), and (5) using $x' = 1.062$, and A_R and τ_0' as fit parameters. Examples of the fits of D_R and α_R are shown in Figs. 11 and 12. The attenuation α_R is a nearly symmetric function of $\log_{10} t$, as expected from Eq. (2). The agreement between the fitted curves and the data for α_R and for D_R is reasonably good. As can be seen in Fig. 12, the curves fitted to α_R show a slightly smaller half width and are shifted with respect to the experimental data. It is not possible to overcome these problems with differently chosen parameters or by fitting the data only for $|T - T_\lambda^s| > 10^{-5}$ K. This same systematic deviation has been observed at SVP and in the mixtures.[2,6] Possibly the division into two additive components according to Eqs. (12) and (13) does not exactly describe the attenuation and dispersion of sound in our temperature and frequency range, or the equations given in Sec. II B do not completely describe the relaxation part of α and D.

In Fig. 10 we also show the maximum relaxation attenuation $\alpha_{R,\max}$ as a function of pressure. These results demonstrate the similar behavior of the strengths of the relaxation and fluctuation attenuation which are of similar magnitude over the entire pressure range, the relaxation attenuation being consistently lower. According to Ref. 21, the ratio $\alpha_F/\alpha_R \propto k_B T_\lambda / F_{\text{sing}} \xi^3$. Here F_{sing} is the singular part of the free energy which is proportional to $t^2 C_{p,\text{sing}} \propto t^{2-\alpha'}$, where α' is the critical exponent of the specific heat. With the scaling law $2 - \alpha' = 3\nu'$ we have $F_{\text{sing}}\, \xi^3 = \text{constant}$, and the ratio α_F/α_R should be universal. This prediction is fulfilled by our data (see Fig. 10).

The consistency between our dispersion and attenuation data is confirmed by the agreement of the parameters A_R (to within about 10%) and τ_0' (to within about 40%) obtained from independent fits of α_R and D_R. The mean values for A_R and τ_0' as a function of pressure are shown in Figs. 13 and 14. They are both independent of pressure within our accuracy, with mean values

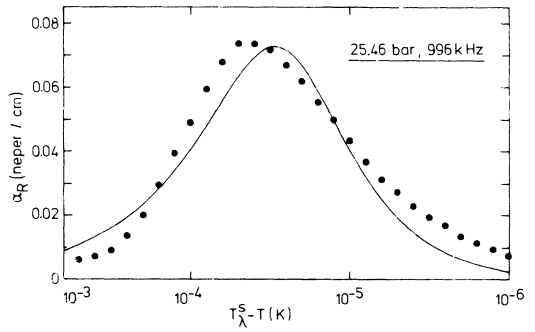

FIG. 12. Relaxation part α_R of the attenuation as a function of $T_\lambda^s - T$ for $P = 25.46$ bar and $\omega/2\pi = 996$ kHz. The data points were determined from continuous measurements and are the difference $\alpha^- - \alpha^+$ of the attenuation measured below and above T_λ^s. The full line is a fit of Eq. (2) with Eqs. (3a) and (5) to the data shown with $x' = 1.062$, and A_R and τ_0' as free parameters.

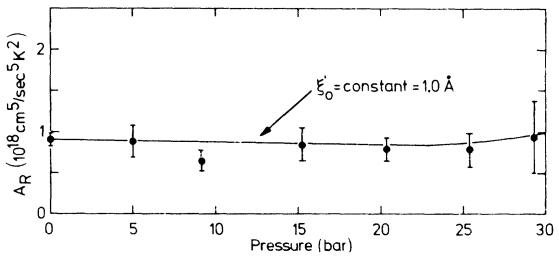

FIG. 13. Amplitude A_R of $\Delta u = u(\infty) - u(0)$ [see Eq. (5)] as a function of pressure. The points are the mean values determined from fits of Eq. (2) with Eqs. (3a) and (5) to the relaxation parts of the attenuation and dispersion at various frequencies. The error bars represent the scatter in the values obtained from the individual fits. The full line is calculated from Eq. (6) assuming a pressure-independent value $\xi_0' = 1.0$ Å.

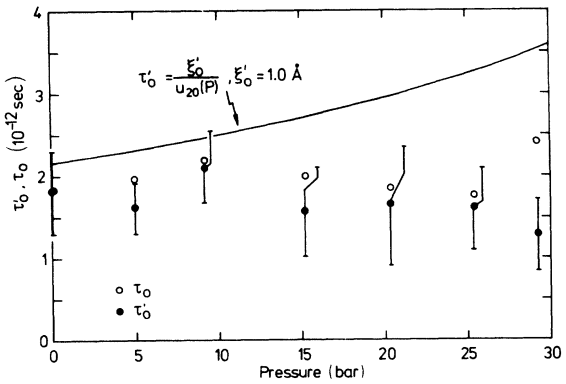

FIG. 14. Amplitude τ_0' of the relaxation time $\tau' = \tau_0' t^{-x'}$ at $T < T_\lambda$, and amplitude τ_0 of the fluctuation time $\tau = \tau_0 t^{-x}$ at $T > T_\lambda$ as a function of pressure. The full points are the mean values from fits of Eq. (2) with Eqs. (3a) and (5) with $x' = 1.062$ to the relaxation part of the attenuation and dispersion at various frequencies. The error bars represent the scatter in the individual fits. The solid line is the computed τ_0' using our determination of $\xi_0' = 1.0$ Å independent of pressure, and the pressure-dependent second sound amplitude $u_{2,0}$ (see Table II). The open circles are the values of τ_0 obtained from the scaling analysis of α and D at $T > T_\lambda$ described in Sec. V C; they are normalized to $\tau_0' = 1.82 \times 10^{-12}$ sec at $P = 0$.

$$A_R = (0.82 \pm 0.08) \times 10^{18} (\mathrm{cm}^5/\mathrm{sec}^5\ \mathrm{K}^2),$$
$$\tau_0' = (1.7 \pm 0.2) \times 10^{-12}\ (\mathrm{sec}). \qquad (14)$$

This behavior contrasts strongly with their concentration dependence in the mixtures, where A_R changes by more than two orders of magnitude, and τ_0' changes by more than one order of magnitude for $0 \leq X_3 \leq 0.52$.[6] Using for the parameters of C_p in Eq. (5) the values given in Ref. 24 instead of the parameters of Ref. 25 changes τ_0' by less than 1%, and A_R by about 3%. Also shown in Fig. 13 are the values calculated for A_R with Eq. (6) using $\xi_0' = 1.0$ Å at all pressures. The agreement with our data is excellent, supporting our analysis as well as the pressure independence of A_R and ξ_0'. The data determine ξ_0' to within 0.05 Å. This value for ξ_0' is in agreement with the amplitude found for the superfluid healing length, 1.2 ± 0.1 Å.[23] But both these values disagree by about a factor of three with the amplitude $\xi_{T,0}'$ of the transverse correlation length, calculated from ρ_s with $\xi_T' = m^2 k_B T / h^2 \rho_s$.[14,19,20] In Fig. 14 we show $\tau_0' = \xi_0' / u_{2,0}(P)$ with $\xi_0' = 1.0$ Å and $u_{2,0}(P)$ from Table II. The observed pressure independence of ξ_0' and τ_0' is inconsistent with the pressure dependence of $u_{2,0}$ if the relaxation time is given by $\tau' = \xi'/u_2$. At the highest pressures, our τ_0' has to be a factor of 2 bigger to remove this descrepancy. We feel that a factor of 2 is outside of our errors. A result $\tau' \neq \xi'/u_2$ has also been obtained in Ref. 38 from hypersonic sound attenuation by Brillouin scattering near T_λ. Also shown in Fig. 14 are values τ_0 obtained from a scaling analysis of the data at $T > T_\lambda$ to be discussed below. These values, too, are independent of pressure to within the errors. For a discussion of the results using equations which include confluent singular terms in t, see the Appendix. These results are identical to the above ones to within the stated uncertainties.

TABLE II. Parameters for $u_2 = u_{2,0} t^{0.387} (1 + u_{2,1} t^{0.5})$, calculated from the data of Ref. 22.

P (bar)	0.05	7.27	12.13	18.06	24.10	29.09
$u_{2,0}$(cm/sec)	4647	4110	3806	3493	3135	2832
$u_{2,1}$	0.004	0.248	0.375	0.525	0.780	1.075

B. Frequency dependence of α and D

If we write for the maximum total attenuation, the maximum of its relaxation part, or the attenuation near T_λ (maximum fluctuation part),

$$\alpha \propto \omega^{1+y}, \qquad (15)$$

we find the exponents y given in Fig. 15.[39] For each of these attenuation values the exponent y is the same (within our errors), and y is independent of pressure, with a value $y = 0.15 \pm 0.03$, except possibly at SVP where our data indicate $y \approx 0.10$. An exponent y slightly larger than zero is in agreement with the result $y \approx 0.15$ of Ref. 2 and $y = 0.10$ for $X_3 = 0$ in data of BP.[6] The exponent y increases up to 0.3 at higher frequencies,[4,7,40] and up to 0.6

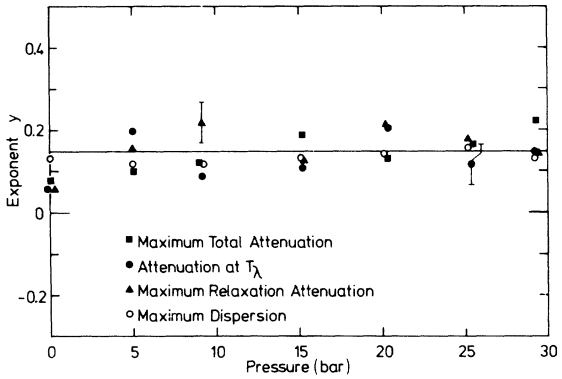

FIG. 15. Exponents y of the frequency dependence of $\alpha \propto \omega^{1+y}$ for the three attenuation values, and of the frequency dependence of the dispersion $u(\omega) - u_\lambda^*(0) \propto \omega^y$. The investigated frequency range is 4.6 kHz $\leq \omega/2\pi \leq 1.0$ MHz. The error bars shown are representative of the uncertainties in all the data. The line at $y = 0.15$ is a guide for the eye only.

in concentrated ^{3}He-^{4}He mixtures.[6,7,8] With the proportionality

$$u(\omega) - u_\lambda^*(0) \propto \omega^y \tag{16}$$

we find the frequency exponents y of the dispersion near T_λ, which are also given in Fig. 15. The obtained values are in very good agreement with the corresponding values for the attenuation. But since y is small, we cannot distinguish between Eq. (16) and $u(\omega) - u_\lambda^*(0) \propto \log_{10}(\omega)$, which is equally compatible with our data. The frequency dependence of the attenuation and dispersion as shown in Fig. 15 is in agreement with $y = \alpha'_{\rm eff}/\nu' \simeq 0.12$ (here α' is an effective exponent of 0.08 for the specific heat in our temperature range).[11,15] But it exceeds the prediction $y \simeq 0.05$ of Ref. 28. For $\omega\tau < 0.1$, where our data are less accurate, they allow the expected hydrodynamic behavior $\alpha \propto \omega^2$ and $D \propto \omega^2$.

C. Scaling of dispersion and attenuation

Our attenuation and dispersion data at all ω and P behave similarly (see Figs. 6–9). Hence, one may expect that by using an appropriate scaling variable the results for all ω and P may collapse onto a single curve which would determine the form of the scaling function f of Eq. (8). Therefore, a more general analysis of our data based on scaling assumptions was performed by fitting them to scaling equations like Eq. (8) with the variable $\omega\tau$, where τ would be a time characterizing the fluctuation process. Recently, this approach has been discussed in detail by BP for the case of sound attenuation and dispersion in ^{4}He and ^{3}He-^{4}He mixtures,[6] and has been applied by Golding[41] to sound attenuation at the ferromagnetic transition of MnP, as well as to sound attenuation in ^{4}He and ^{3}He-^{4}He mixtures at higher frequencies than used here in Refs. 4, 7, and 8. Here we proceed as described in Ref. 6.

1. Attenuation at $T > T_\lambda$

The data above T_λ where only fluctuations contribute will be analyzed. The exponent and amplitude of the characteristic time $\tau = \tau_0 t^{-x}$ are determined independently. All data at $T > T_\lambda$ are normalized to their values near T_λ, which means at large $\omega\tau$. This normalization removes the frequency factor ω^{1+y} from α; a normalization at $\omega\tau = 1$ gives the same results.[6,39] The data at all frequencies and at one pressure were plotted as a function of $\omega\tau_0 t^{-x}$ with $\tau_0 = 2 \times 10^{-12}$ sec and for various x in the range $0.8 \leq x \leq 1.4$. This was repeated for each pressure. These plots show that the best agreement of the data measured at various ω is obtained for $x = 1.1 \pm 0.1$ for all investigated pressures. Within the given resolution we cannot distinguish whether the best matching of the data to one curve for each pressure is obtained for $x = 1.1$ or $x = x' = \nu' + w = 1.062$, where ν' and w are the critical exponents of the correlation length and of the velocity of second sound at $T < T_\lambda$ [see Eqs. (3a) and (3b)]. We use $x = 1.062$ in the following.

Now, τ_0 is treated as a free parameter. We plot the data for all ω and all P versus $\omega\tau_0 t^{-1.062}$ with values of τ_0 so that the data for all pressures, too, collapse onto one curve. The result is shown in Fig. 16. Within deviations of less than 10% the data points for all ω and P, for the investigated ranges, collapse onto a single curve. The deviation of the data points is random without correlation to ω, $\omega\tau$, or P. The values of τ_0 for each pressure, giving the best matching of the individual curves, measured at different ω and P, are shown in Fig. 14 (normalized to $\tau_0'(P = 0.06) = 1.82 \times 10^{-12}$ sec which has been obtained from our analysis in Sec. V A). Within the errors, the amplitude τ_0 of the order parameter fluctuation time $\tau = \tau_0 t^{-x}$ determined from this scaling analysis at $T > T_\lambda$ agrees with the relaxation time amplitude τ_0' determined in Sec. V A from the fit of the relaxation part of the attenuation and dispersion at $T < T_\lambda$. The time τ, too, has a pressure-independent amplitude, and τ_0/τ_0', of course, is universal. We conclude that the critical attenuation α_F of first sound at $T > T_\lambda$ in pressurized ^{4}He and for 65 kHz $\leq \omega/2\pi \leq 1$ MHz can be scaled by Eq. (8) over at least four decades in $\omega\tau$. The attenuation normalized near T_λ (or at $\omega\tau = 1$) is a function of $\omega\tau$ only, thus including the dependence on t, ω, and P. The amplitude of the characteristic time τ as well as its

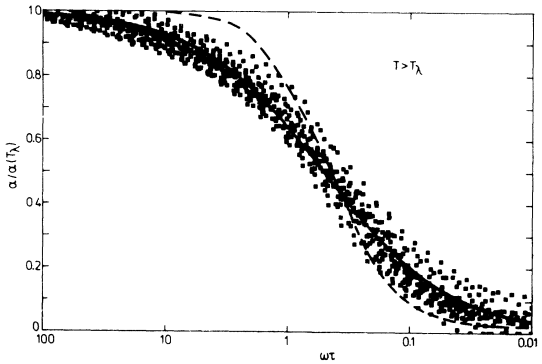

FIG. 16. Scaling plot of the critical attenuation α at $T > T_\lambda$ normalized to $\alpha(T_\lambda)$ for 65 kHz $\leq \omega/2\pi \leq 1.0$ MHz, and for all investigated pressures versus the scaling variable $\omega\tau$. If Eq. (8) holds, all points should lie on the same curve. For the time $\tau = \tau_0 t^{-x}$ we used $x = 1.062$ and τ_0 as given in Fig. 14. The full line is the function $f_F = (\omega\tau)^{1-y}/[c + (\omega\tau)^{1-y}]$ with $y = 0.15$ and $c = 0.52$ discussed in the text. The dashed line is a theoretical calculation by Kroll (Ref. 28) (see text).

critical exponent which we find for the scaled critical attenuation at $T > T_\lambda$ agree to within the given errors with the amplitude and the critical exponent of the relaxation time τ' at $T < T_\lambda$, possibly to within a factor which is independent of t, ω, and P. This unknown factor arises because the scaling gives only relative values for τ_0. The same conclusions have been obtained by BP for the attenuation of sound in ^{3}He-^{4}He mixtures.[6] Thus, there is a unique time scale throughout the critical region.

The scaling function $f(\omega\tau)$ can be determined from the data of Fig. 16. A function which fits the data well and has the correct asymptotic limits is shown in Fig. 16, and is given by

$$f(\omega\tau) = (\omega\tau)^{1-y}/[c + (\omega\tau)^{1-y}], \tag{17}$$

with $y = 0.15$. By fitting the attenuation to various functions $f(\omega\tau)$ with y varied, we find that the data can be represented for $0 \lesssim y \lesssim 0.3$. A function like $\omega\tau/(c + \omega^2\tau^2)$ is excluded by the data. The function given by Eq. (17) best fits the data with a constant $c = (0.52 \pm 0.01)(\tau_0/\tau_0')^{1-y}$. The factor $(\tau_0/\tau_0')^{1-y}$ is necessary because the scaling procedure provides only relative values of τ_0. BP found that Eq. (17) represented their attenuation data for $X_3 \leq 0.2$ with $c = (0.55 \pm 0.01)(\tau_0/\tau_0')^{1-y}$, and $y = 0.10$.[42] It is clear that one function is able to scale all the attenuation data for $T > T_\lambda$, 65 kHz $\leq \omega/2\pi \leq 1$ MHz, for at least $X_3 \leq 0.2$, and for all P along the λ lines. This provides strong verification that pressure and concentration of ^{3}He are inert variables for the superfluid transition, as predicted by universality.[16]

Recently, Kroll has calculated the critical sound attenuation near T_λ.[28] Similarly to Kawasaki,[15] he uses mode-mode coupling theory to calculate α_F due to fluctuations in terms of the order parameter and entropy correlation functions. The correlation functions are then calculated in the framework of renormalization group theory.[43] The only correction terms explicitly included in the calculation are those of the specific heat.[28] The results are considered to be more trustworthy at small $\omega\tau$, and there to be correct to within about 30% according to Ref. 28. The obtained result is $\alpha \propto \omega^{1+y} f^*(\omega\tau)$ with $y \simeq 0.05$. The resulting scaling function has been calculated numerically,[28] and is plotted in Fig. 16. It agrees with the experimental data to within the mentioned accuracy but the calculated dependence of α on $\omega\tau$ for $0.1 < \omega\tau < 10$ is too strong compared to our data, and y is smaller than our values, (see Fig. 15).

2. *Dispersion at $T > T_\lambda$*

The dispersion as a function of $\omega\tau$ is plotted in Fig. 17. We used τ_0 from the scaling analysis of the attenuation. We have not normalized the data

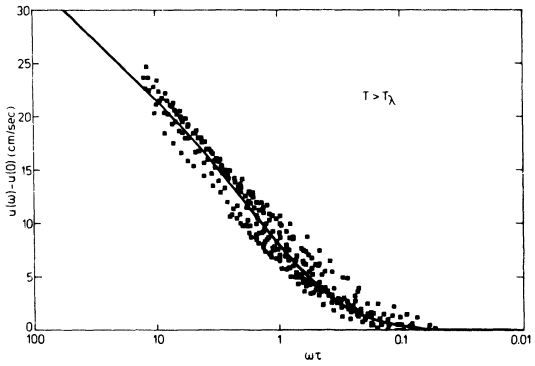

FIG. 17. Scaling plot of the critical dispersion D at $T > T_\lambda$ and for $\omega/2\pi = 200$ kHz and 1.0 MHz, for $|T_\lambda^s - T| \geq 5\ \mu$K and all investigated pressures versus the scaling variable $\omega\tau$. If Eq. (8) holds, all points should lie on the same curve. The time τ for each pressure was determined from the scaling of the attenuation (Fig. 16). No normalization for the frequencies is applied; data for $P = 0.06$, 5.01, 9.21, 15.24, 20.38, 25.46, and 29.33 bar were multiplied by $D_0(P) = 1$, 1.05, 0.87, 0.77, 0.50, and 0.67, respectively. The line is given by Eq. (18) with $y = 0.15$.

near T_λ but matched the data as best as is possible with the factors $D_0(P) = 1$, 1.05, 0.87, 0.77, 0.50, and 0.67 for $P = 0.06$, 5.01, 9.21, 15.24, 20.38, 25.46, and 29.33 bar, respectively. The small change of D_0 with P indicates the weak influence of P on dispersion (and attenuation). Only data near 200 kHz and 1 MHz and for $|T - T_\lambda^s| > 5\ \mu$K have been analyzed. The scaled dispersion does not approach an asymptotic value in the investigated $\omega\tau$ range.

A scaling function that represents our data, and gives the correct asymptotic behavior at large and small $\omega\tau$ is

$$D = D_1\omega^2\tau^2/(d + \omega\tau)^{2-y}, \tag{18}$$

with

$$D_1 = [16.7/D_0(P)](\tau_0'/\tau_0)^y \text{ cm/sec},$$

$$d = 0.48(\tau_0/\tau_0'),$$

$D_0(P)$ as given above, and $y = 0.15$. This is shown as the solid line in Fig. 17, and agrees again with the scaling function for D given by BP.[6]

VI. SUMMARY AND CONCLUSIONS

We have performed a systematic study of sound propagation at frequencies $\omega/2\pi \leq 1$ MHz in pressurized ^{4}He close to the λ transition. By using a sample chamber of 0.5-cm height only, gravity effects were kept very small. The temperature and pressure resolution and regulation were $\Delta T/T \simeq 3 \times 10^{-7}$ and $\Delta P/P \simeq 10^{-7}$, respectively. From

the data taken at $\omega/2\pi \leq 7.4$ kHz, we determined the thermodynamic velocity of sound, as well as the related parameters $(\partial S/\partial P)_\lambda$ and $(\partial V/\partial P)_\lambda$ along the λ line.

The attenuation α and dispersion D are only weakly pressure dependent. It is shown, that α and D can be represented as arising from a relaxation process at $T < T_\lambda$, and critical order parameter fluctuations on both sides of the transition. The strength A_R of the relaxation process is independent of pressure (to with 10%). From A_R we calculate a pressure independent amplitude of the correlation length (at $T < T_\lambda$), $\xi_0' = 1.0 \pm 0.05$ Å. This result is in agreement with the pressure-independent amplitude of the healing length in He II, $\xi_{H,0}' = 1.2 \pm 0.1$ Å reported in Ref. 23. The transverse correlation length determined from ρ_s with the relation $\xi_T' = m^2 k_B T/\hbar^2 \rho_s$,[14,19,20] on the other hand has an amplitude of $\xi_{T,0}' = (3.24 \pm 0.08)$ Å, again independent of pressure within the given limits.[44] $\xi_{T,0}'$ can also be determined from the universal quantity $\xi_{T,0}' A'^{1/3} = 0.36$,[20] where A' is the amplitude of the specific heat. This equation gives a value of $\xi_{T,0} = 4$ Å. The values of A_R calculated with $\xi_{T,0}$ instead of ξ_0' differ by a factor of about 30 from our measured A_R. It therefore seems that the transverse correlation length is neither equal to the characteristic length determining the Landau-Khalatnikov relaxation nor to the healing length near a boundary.

According to universality[16] the ratio of amplitudes of all these lengths has to be pressure independent, and all these lengths should have the same critical exponent according to scaling.[30] Both predictions are in agreement with experimental results.

Assuming a universal critical exponent x' for the relaxation time $\tau' = \tau_0' t^{-x'}$, we found its amplitude τ_0' to also be pressure independent. These results disagree with the pressure dependence of the amplitude of the velocity of second sound $u_{2,0}$, if the relation $\tau' = \xi'/u_2$ is correct.

In the Appendix we show that our results are not changed if confluent singular terms in t are included in the used equations.

The data for $T > T_\lambda$ where only fluctuations contribute are analyzed with scaling functions of $\omega\tau$. We find that the critical attenuation, e.g., can be scaled by the function $f = (\omega\tau)^{1-y}/[c + (\omega\tau)^{1-y}]$ for all investigated ω and P, and for $10^2 \geq \omega\tau \geq 10^{-2}$. Our data and this scaling analysis allow $0 \leq y \leq 0.3$. The scaling function agrees with hydrodynamics at $\omega\tau \ll 1$ for $\alpha \propto \omega^{1+y} f$. The resulting order parameter fluctuation time for $T > T_\lambda$, $\tau = \tau_0 t^{-x}$, has the same temperature and pressure dependence as the relaxation time τ' at $T < T_\lambda$. Hence these two times differ by at most a constant multiplicative factor, and there exists a unique time scale throughout the critical region, as predicted by dynamic scaling. In a corresponding analysis it is shown that the dispersion, too, can be scaled at $T > T_\lambda$ for the investigated t, ω, and P ranges. The scaling functions determined from our data are identical in form to those determined from the ^{3}He-^{4}He mixture data.[6] For $T < T_\lambda$, the data are represented by the scaling function, determined from the data for the fluctuation contribution at $T > T_\lambda$, plus the contribution from order parameter relaxation.

In the critical region for $\omega\tau \gtrsim 1$, attenuation and dispersion behave as $\alpha \propto \omega^{1+y}$ and $D \propto \omega^y$, with $y = 0.15 \pm 0.03$ at all pressures, possibly except at SVP where the data are better fit if $y \simeq 0.10$.

With the data obtained here at $\omega/2\pi \leq 1$ MHz for pressurized ^{4}He and obtained previously for ^{3}He-^{4}He mixtures,[6] as well as the data at higher frequencies,[2,4,7,8,40] we have detailed and systematic information on sound propagation near the superfluid transition. First steps towards a microscopic theory—to which we compared our results—have been taken recently.[28] Still more effort on the theoretical part seems to be necessary to arrive at a comprehensive interpretation of the data on both sides of the transition as well as for all investigated ω, P, and X_3 ranges.

APPENDIX: INCLUSION OF CONFLUENT SINGULAR TERMS

Detailed measurements of the velocity of second sound and of the superfluid density,[22] the specific heat,[24] and the thermal expansion coefficient[25] of pressurized ^{4}He near T_λ have demonstrated that these and other properties cannot be represented in the experimentally accessible temperature range near T_λ by pure power laws without conflict with theoretical predictions of scaling and universality. A confluent singularity in addition to the leading singularity had to be included to render a consistent interpretation of the data. Both parameters of Eqs. (2), Δu and τ', can contain correction terms. We have therefore analyzed our data with equations including the next-order term in t to check its influence on our results. For this purpose we expressed ξ' in terms of ρ_s by using the theoretical prediction[14,19,20]

$$\xi' \propto T \rho_s^{-1} . \tag{A1}$$

This universal proportionality has been confirmed experimentally by Ihas and Pobell for the superfluid healing length ξ_H',[23] from which ξ' should only differ by a constant multiplicative factor according to scaling.[30] The equation for the superfluid density, as determined from second sound velocity,[22] is

$$\rho_s/\rho = k(P)t^{\zeta}[1 + a(P)t^{z}], \tag{A2}$$

with universal exponents $\zeta = 0.675$ and $z = 0.5$.[22,25] With Eqs. (4), (6), (A1), and (A2) we find

$$\Delta u = A_R C_p(T)^{-2} t^{3\zeta-2}[1 + (3 + 2z/\zeta)at^{z}]$$
$$= A_R C_p(t)^{-2} t^{0.026}(1 + 4.48at^{0.5}). \tag{A3}$$

To also determine τ' with a confluent singularity, we express the velocity of second sound near T_λ as

$$u_2 = u_{2,0}(P)t^{w}[1 + u_{2,1}(P)t^{z*}]. \tag{A4}$$

An exponent of $w = 0.387$ has been shown to represent the data well at SVP where $u_{2,1}$ is only 4×10^{-3}.[29] This exponent agrees approximately with $u_2 \propto \rho_s^{1/2} C_p^{-1/2}$ and $w = \zeta/2 + 0.04$, where an effective exponent of 0.08 for C_p in the temperature range of interest has been used. For the exponent of the correction term we use $z^* = 0.5$. The two exponents w and z^* probably have no theoretical significance, and serve only to represent the data. We obtained the amplitudes $u_{2,0}$ and $u_{2,1}$, as given in Table II, by fitting the above equation to the data of Ref. 22.

With Eqs. (3b), (A1), and (A4) we have

$$\tau' = \tau_0' t^{-\zeta-w}(1 - at^{z} - u_{2,1}t^{z*})$$
$$= \tau_0' t^{-1.062}[1 - (a + u_{2,1})t^{0.5}], \tag{A5}$$

with

$$\tau_0' = \xi_0'/u_{2,0}. \tag{A6}$$

The analysis with the above equations was performed in analogy to the analysis without confluent singular terms as discussed in the text. The results show that τ_0' is decreased by less than 1% and A_R is decreased by at most 3% if the confluent singular terms are included. These changes are smaller than the scattering of the parameters from runs performed at different ω or obtained from α_R and D_R, e.g. They are smaller than the stated uncertainties.

In addition, a third analysis has been performed, avoiding Eq. (A4) for u_2, and expressing τ' only in terms of ρ_s and C_p,

$$\tau' = \xi'/u_2 = \tau_0^{*\prime} C_p(t)^{1/2} t^{-3\zeta/2}(1 - \tfrac{3}{2}at^{y} - \tfrac{1}{2}kt^{\zeta})$$
$$= \tau_0^{*\prime} C_p^{1/2} t^{-1.013}(1 - \tfrac{3}{2}at^{0.5} - \tfrac{1}{2}kt^{0.675}),$$

with

$$\tau_0^{*\prime} = m^2 k_B T^{1/2}/\hbar^2 \rho S k^{3/2}.$$

The values obtained for A_R agree to within 3% with those from the other two analyses, and $\tau_0^{*\prime}$ again is pressure independent to within about 5%, having a mean value of 2.1×10^{-16} sec^2 K$^{1/2}$ g$^{-1/2}$ cm^{-1}.

ACKNOWLEDGMENT

We gratefully acknowledge discussions with Dr. D. Kroll, a critical reading of the manuscript by Professor J. Mehl, and technical assistance by J. Hanssen.

*Present address: University of Maine, Dept. of Physics and Astronomy, Orono, Me. 04473.

[1]M. Barmatz and I. Rudnick, Phys. Rev. 170, 224 (1968).
[2]R. D. Williams and I. Rudnick, Phys. Rev. Lett. 25, 276 (1970); R. D. Williams, thesis (University of California, 1970) (unpublished).
[3]W. C. Thomlinson and F. Pobell, Phys. Rev. Lett. 31, 283 (1973).
[4]A. Ikushima and K. Tozaki, in *Proceedings of the Fourteenth International Conference on Low Temperature Physics*, edited by M. Krusius and M. Vuorio (North-Holland, Amsterdam, 1975), Vol. 1; K. Tozaki and A. Ikushima, Phys. Lett. A 59, 458 (1977).
[5]C. Buchal, F. Pobell, and W. C. Thomlinson, Phys. Lett. A 51, 19 (1975).
[6]C. Buchal and F. Pobell, Phys. Rev. B 14, 1103 (1976).
[7]A. Ikushima, D. B. Roe, and H. Meyer, *Proceedings of the Second International Conference on Phonon Scattering in Solids*, edited by L. J. Challis, V. W. Rampton, and A. F. G. Wyatt (Plenum, New York, 1976).
[8]D. B. Roe, G. Ruppeiner, and H. Meyer, J. of Low Temp. Phys. 27, 747 (1977).
[9]L. D. Landau and I. M. Khalatnikov, Dokl. Akad. Nauk SSSR 96, 469 (1954).
[10]V. L. Pokrovskii and I. M. Khalatnikov, Zh. Eksp. Teor. Fiz. Pis'ma Red. 9, 225 (1969) [JETP Lett. 9, 149 (1969)]; I. M. Khalatnikov, *ibid.* 57, 489 (1969) [*ibid.* 30, 268 (1970)].
[11]P. C. Hohenberg, in *Proceedings of the International School "Enrico Fermi," Course LI*, edited by M. S. Green (Academic, New York, 1971); we neglect a constant, unknown factor of order unity in Eq. (4.13) of this reference corresponding to our Eq. (4).
[12]D. G. Sanikidze, Zh. Eksp. Teor. Fiz. 66, 714 (1974) [Sov. Phys.-JETP 39, 349 (1974)]; a square is missing on $(\partial S/\partial P)_\lambda$ in the last term of Eq. (24) in this reference.
[13]R. A. Ferrell, N. Menyhard, H. Schmidt, F. Schwabl, and P. Szepfalusy, Ann. Phys. (N.Y.) 47, 565 (1968); J. Swift and L. P. Kadanoff, *ibid.* 50, 312 (1968).
[14]B. I. Halperin and P. C. Hohenberg, Phys. Rev. Lett. 19, 700 (1967); Phys. Rev. 177, 952 (1969).
[15]K. Kawasaki, Phys. Lett. A 31, 165 (1970); Int. J. Magn. 1, 171 (1971).
[16]L. P. Kadanoff, in Ref. 11; R. B. Griffiths, Phys. Rev. Lett. 24, 1479 (1970); D. Jasnow and M. Wortis, Phys. Rev. 176, 739 (1968).
[17]E. Brézin, J. C. LeGuillou, and J. Zinn-Justin, Phys. Lett. A 47, 285 (1974).
[18]D. Stauffer, M. Ferer, and M. Wortis, Phys. Rev. Lett. 29, 345 (1972).
[19]B. I. Halperin, P. C. Hohenberg, and E. D. Siggia, Phys. Rev. B 13, 1299 (1976).
[20]P. C. Hohenberg, A. Aharony, B. I. Halperin, and

E. D. Siggia, Phys. Rev. B 13, 2986 (1976); C. Bervillier, *ibid.* 14, 4964 (1976).
[21]D. Stauffer (private communication); and unpublished.
[22]D. Greywall and G. Ahlers, Phys. Rev. Lett. 28, 1251 (1972); Phys. Rev. A 7, 2145 (1973).
[23]G. G. Ihas and F. Pobell, Phys. Rev. A 9, 1278 (1974).
[24]G. Ahlers, Phys. Rev. A 3, 696 (1971); 8, 530 (1972).
[25]K. H. Mueller, F. Pobell, and G. Ahlers, Phys. Rev. Lett. 34, 513 (1975); Phys. Rev. B 14, 2096 (1976).
[26]G. Ahlers, Phys. Rev. 182, 352 (1969).
[27]G. Ahlers, J. Low Temp. Phys. 1, 609 (1969).
[28]D. Kroll (private communication); and unpublished.
[29]G. Ahlers, Phys. Rev. A 10, 1670 (1974).
[30]B. Widom, J. Chem. Phys. 43, 3892 (1965); 43, 3898 (1965); L. P. Kadanoff, Physics (N.Y.) 2, 263 (1966); B. D. Josephson, Phys. Lett. 21, 608 (1966).
[31]G. Ahlers, Phys. Rev. 171, 275 (1968).
[32]Model CR 2500 L, Cryo Cal Inc., Riviera Beach, Fla.
[33]More precise figures for the investigated frequencies (in kHz) in the cylindrical resonator are 197, 1010 at 0.06 bar; 103, 206, 570, 1005 at 5.01 bar; 84.4, 197, 565, 987 at 9.21 bar; 92.7, 185, 620, 1022 at 15.24 bar; 65.6, 196, 592, 1018 at 20.38 bar; 68.6, 205, 549, 996 at 25.46 bar; 70.1 211, 563, 1020 at 29.33 bar, in addition to the low-frequency second harmonic f_{T2} in the torus resonator (see text).
[34]A tabulation of velocity, dispersion, and attenuation data can be obtained on request.
[35]H. A. Kierstaed, Phys. Rev. 162, 153 (1967).
[36]C. Van Degrifft, thesis (University of California, 1974) (unpublished).
[37]J. Maynard, Phys. Rev. B 14, 3868 (1976).
[38]F. Vidal, J. A. Tarvin, and T. J. Greytak, Bull. Am. Phys. Soc. 21, 353 (1976).
[39]The same exponents y as for $\alpha(T \simeq T_\lambda) \propto \omega^{\frac{1}{2}y}$ are found for $\alpha^+(\omega\tau = 1) \propto \omega^{\frac{1}{2}y}$.
[40]D. E. Commins and I. Rudnick, in *Proceedings of the Thirteenth International Conference on Low Temperature Physics*, edited by K. D. Timmerhaus, W. J. O'Sullivan, and E. F. Hammel (Plenum, New York, 1974), Vol. 1.
[41]B. Golding, Phys. Rev. Lett. 34, 1102 (1975).
[42]For $0.2 < \chi_3 \leq 0.52$, the data were scaled better by the function $f(\omega\tau) = \omega\tau/(c + \omega\tau)$ (Ref. 6). But this function does not approach the hydrodynamic behavior.
[43]See, for instance, K. G. Wilson and J. Kogut, Phys. Rep. 12C, 75 (1974); E. Brézin, D. J. Wallace, and K. G. Wilson, Phys. Rev. B 7, 232 (1973).
[44]These values for $\xi'_{T,0}$ are obtained if the ρ_s/ρ data of Ref. 22 are used.